Numerical Instability Resulting from Infrequent Calculation of Radiative Heating

OLIVIER PAULUIS* AND KERRY EMANUEL

Program in Atmospheres, Oceans, and Climate, Massachusetts Institute of Technology, Cambridge, Massachusetts

(Manuscript received 4 February 2003, in final form 18 July 2003)

ABSTRACT

Owing to its relative expense, radiative heating is often not calculated for every time step in numerical simulations of the atmosphere. This is justified when the radiation field evolves slowly in comparison to the atmospheric flow. However, when the effects of variable water vapor and clouds are taken into account, the radiation field can change rapidly, and the finite time between calls to the radiation scheme can introduce a destabilizing time lag. In the worst case, this lag gives rise to an exponential numerical instability with a growth rate proportional to the time interval between radiative calculations. In less drastic circumstances, in which the radiation would damp oscillations of the real system, numerical instability occurs when the time interval between calls to the radiation scheme exceeds a critical value that depends on the Doppler-shifted natural oscillation frequency and the radiative damping rate. It is shown that this type of instability occurs in a single-column model as well as in an idealized general circulation model. The critical frequency at which the radiative heating rate should be computed is found to depend on several factors, including the large-scale circulation and the model resolution. Several potential remedies are discussed.

1. Introduction

The calculation of radiative transfer is often among the most time-consuming tasks in numerical integrations of atmospheric models. It has become common practice to calculate radiative heating at intervals of many time steps and, in some cases, to calculate it on a coarser mesh than is used for the model's dependent variables. The radiative fluxes are then held fixed until the next time step, or simple corrections are made at every time step until the radiation is next calculated. For example, in the current implementation of the weather forecast model of the European Centre for Medium-Range Forecasts (ECMWF), the radiation scheme is invoked every 3 h. Subsequent to each call to the radiation scheme, the shortwave fluxes are corrected at each time step according to the cosine of the solar zenith angle, while the longwave fluxes are held fixed in time until the next call to the radiation scheme. The full radiation calculation is performed on a coarse grid and interpolated to the standard grid using a cubic interpolation scheme (Morcrette 2000).

There is some evidence that the temporal resolution of the radiative transfer can affect model fields. Morcrette (2000) showed, using the ECMWF model, that while temporal resolution of radiation had little effect on standard measures of forecast skill at 10 days, it had noticeable effects on seasonal forecasts and, especially, on model climate sensitivity. Charlock et al. (1988) noted that climate simulations using the National Center for Atmospheric Research Community Climate Model (CCM), in which radiation is calculated every 12 h, exhibit more variability of outgoing longwave radiation than is evident in satellite-based measurements. A detailed analysis of the effects of infrequent calculation of radiation on integrations using a cloud-resolving cumulus ensemble model was undertaken by Xu and Randall (1995). They showed that increasing the time intervals between calls to the radiation scheme leads to increasing distortion in the cloud vertical velocities and domain-averaged precipitation.

In this paper, the sensitivity of numerical integrations to the frequency with which radiation is calculated is further explored using both simple linear models and a single-column model with sophisticated convection and radiation subroutines. In the following section, we use simple linear models to investigate numerical instabilities related to lagged radiation and to examine the character of the distortions that occur even in the stable regime, when the time interval between application of radiative damping is not very subcritical. The stability

* Current affiliation: Atmospheric Oceanic Sciences Program, Princeton University, Princeton, New Jersey.

Corresponding author address: Olivier Pauluis, NOAA/GFDL, Princeton Forrestal Campus, U.S. Rte. 1, P.O. Box 308, Princeton, NJ 08542-0308.
E-mail: omp@gfdl.gov

criteria are tested and the effects of infrequent calculation of radiation are further explored using the single-column model in section 3, and in a general circulation model in section 4. Possible remedies are described in section 5.

2. Linear models and stability criteria

a. General case

Here we consider a linear system containing neutral oscillations, in which the addition of "radiation" changes the frequency of the oscillations or introduces some damping. This system is described by the coupled equations

$$\frac{dM}{dt} = -T, \tag{1}$$

$$\frac{dT}{dt} = N^2M + R, \tag{2}$$

$$R = \alpha M_n - \beta T_n, \tag{3}$$

where N is the oscillation frequency in the absence of radiation (R), and M_n and T_n are the values of M and T at the discrete time step n. Although this is not meant to be a physical system, we have in mind an atmosphere in which the convective mass flux (M) is reduced by increased the upper-tropospheric temperature (T) and the temperature is in turn increased by convective mass flux and by radiation (R). The constants α and β control the amplitude and phase of the radiation and result either in an increased frequency (for $\alpha > 0$) or in a damping (for $\beta > 0$) of the oscillation.

When the radiation given by (3) is evaluated continuously in time, then the solution of (1)–(3) is

$$M = e^{-\beta t/2}(M_0 \cos\omega t + \chi \sin\omega t), \tag{4}$$

$$T = e^{-\beta t/2}\left[T_0 \cos\omega t + \left(M_0 + \frac{1}{2}\alpha\chi\right)\sin\omega t\right], \tag{5}$$

where

$$\omega = \sqrt{N^2 + \alpha - \frac{\beta^2}{4}} \quad \text{and} \quad \chi = \frac{\beta M_0}{2\omega} - \frac{T_0}{\omega}.$$

This system behaves as a damped oscillator as long as $N^2 + \alpha - \beta^2/4 > 0$.

Now consider the system in which R is evaluated at discrete time steps, as given by (3). Eliminating T between (1) and (2), and using (3), gives

$$\frac{d^2M}{dt^2} + N^2M = -\alpha M_n - \beta\left(\frac{dM}{dt}\right)_n \tag{6}$$

in which the right-hand side is held constant over each time interval between $t = n\tau$ and $t = (n + 1)\tau$. The solution of (6) valid at time t where t is between time $t = n\tau$ and time $t = (n + 1)\tau$ is

$$M(t) = M_n[-\delta + (1 + \delta)\cos N(t - n\tau)] + \{-\varepsilon[1 - \cos N(t - n\tau)] + \sin N(t - n\tau)\}\frac{1}{N}\left(\frac{dM}{dt}\right)_n, \tag{7}$$

where $\delta = \alpha/N^2$ and $\varepsilon = \beta/N$. Here τ is the time interval between two calculations of the radiative heating rates. At $t = (n + 1)\tau$ this becomes

$$M_{n+1} = [-\delta + (1 + \delta)\cos N\tau]M_n + [-\varepsilon(1 - \cos N\tau) + \sin N\tau]\frac{1}{N}\left(\frac{dM}{dt}\right)_n. \tag{8}$$

If we differentiate (7) with time and evaluate the result at $t = (n + 1)\tau$, we find that

$$\left(\frac{dM}{dt}\right)_{n+1} = [-(1 + \delta)\sin N\tau]NM_n + [-\varepsilon \sin N\tau + \cos N\tau]\left(\frac{dM}{dt}\right)_n. \tag{9}$$

Now, combining (8) and (9) gives the difference equation

$$M_{n+2} + [\delta - (2 + \delta)\cos N\tau + \varepsilon \sin N\tau]M_{n+1} + [1 + \delta(1 - \cos N\tau) - \varepsilon \sin N\tau]M_n = 0. \tag{10}$$

The solution of (10) has the general form

$$M_n = c_1 r_1^n + c_2 r_2^n, \tag{11}$$

where c_1 and c_2 are constants determined by the initial condition and r_1 and r_2 are given by

$$r = \frac{-b \pm \sqrt{b^2 - 4c}}{2}, \tag{12}$$

with $b = \delta - (2 + \delta)\cos N\tau + \varepsilon \sin N\tau$ and $c = 1 + \delta(1 - \cos N\tau) - \beta \sin N\tau$.

According to (11), M will amplify if $|r_1| > 1$ and/or $|r_2| > 1$. There are thus four possibilities, according to whether or not each root is greater than 1 or less than -1, also taking into account the possibility that the argument of the square root is negative.

b. Undamped oscillator

For $\beta = \varepsilon = 0$, the continuous system is a linear oscillator in which the radiation modifies the natural frequency of the oscillator. When radiation acts to increase the natural frequency ($\alpha > 0$), the discretized system is unstable for all values of τ that are not an integer multiple of $2\pi/N$. In the limit of small τ, the leading terms in (12) are

$$r = 1 \pm i\delta^{1/2}N\tau - \delta/4\ N^2\tau^2 + O(N^3\tau^3). \tag{13}$$

The norm is

$$|r| = 1 + \delta/4\ N^2\tau^2 + O(N^3\tau^3). \tag{14}$$

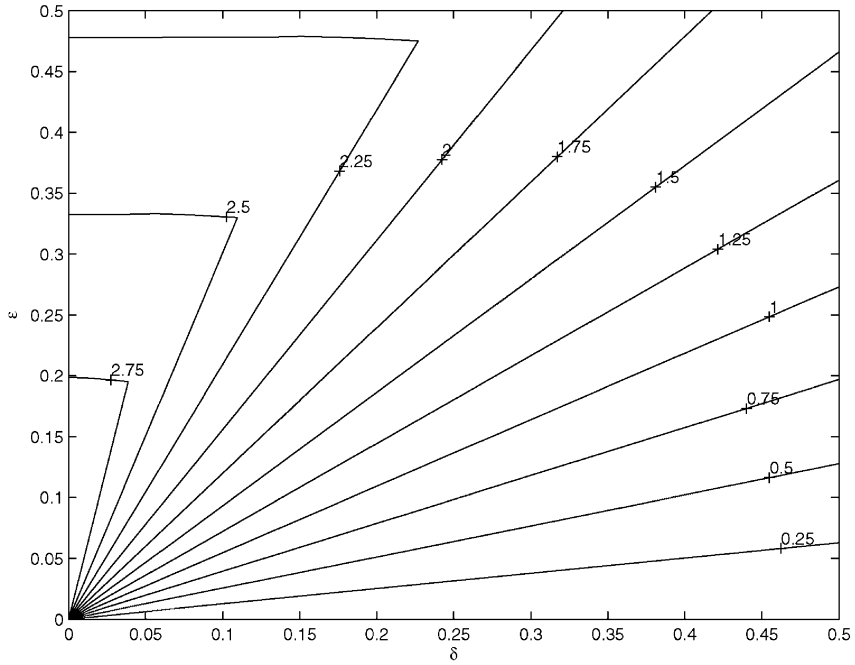

FIG. 1. Critical value of $N\tau$ between radiation calls as function of δ (horizontal axis) and ε (vertical axis).

In the limit of small τ, the system (1)–(3) exhibits a growing oscillation. The frequency converges toward the frequency of the continuous problem $(1 + \delta)^{1/2}N$, but the solutions have an equivalent growth rate of $\frac{1}{4}\alpha\tau$.

When the radiation acts to increase the frequency of the oscillator in the continuous case ($\alpha > 0$), the neutral oscillator is destabilized for any value of the time interval over which the radiation is updated, with the exception of a set of special values of $N\tau$. Conversely, when the radiation acts to reduce the frequency of the internal oscillator in the continuous case, infrequent calculations of the radiation stabilize the neutral oscillator.

c. Damped oscillator

Suppose instead that the radiation tends to damp temperature perturbations (taking $\alpha = 0$ and $\beta > 0$), so that the continuous system is a linear damped oscillator. The solutions of the discretized system are given by (11), with

$$r = \cos(N\tau) - \frac{\varepsilon}{2}\sin(N\tau) \pm \sqrt{\sin(N\tau)\left\{\varepsilon[1 - \cos(N\tau)] + \sin(N\tau)\left(\frac{\varepsilon^2}{4} - 1\right)\right\}}. \quad (15)$$

A sufficient condition for instability, ensuring that $|r| > 1$, is

$$\tau > \tau_c = \frac{2}{N}\tan^{-1}\left(\frac{N}{\beta}\right). \quad (16)$$

Here we will refer to τ_c as the critical value for the time interval, albeit it is only as sufficient value for the instability. Several limiting cases are of interest. First, in the limit of the vanishing oscillation frequency, when the exact solution (1)–(3) is simple exponential decay, (16) gives

$$\lim_{N\to 0} \tau_c = \frac{2}{\beta}, \quad (17)$$

showing that even in the absence of any oscillations, the interval between calls to the radiation scheme must not exceed twice the radiative damping time scale. Second, in the limit of a natural oscillation period much shorter than the radiative damping time scale, we have

$$\lim_{\varepsilon\to 0} \tau_c = \frac{\pi}{N}. \quad (18)$$

This implies that the radiation scheme must be called at intervals no longer than half the period of the (fastest) natural oscillation of the system in this limit. In most of the atmospheric models of which the authors are aware, the radiative time scales are much longer than the relevant dynamical time scales, so that, in practice, the limit given by (18) is usually approached.

Figure 1 shows the critical value of $N\tau_c$ at which the system (1)–(3) first becomes unstable as a function of

the two nondimensional parameters δ and ε. We observe that $N\tau_c$ is smaller than π, indicating that (18) yields only an upper bound for τ_c and does not guarantee stability. In agreement with the discussion in section 2b, the worse case occurs for an accelerated oscillator, which is unstable for any value of the time interval between radiations.

These examples illustrate how infrequent radiation calls can destabilize an internal oscillator. In a linear oscillator, the time tendency of a given variable is out of phase with this variable. By freezing the ''radiative heating'' between the radiation calls, one introduces a time lag in the heating rate. When this time lag results in a positive correlation between ''temperature'' and radiative heating, the oscillator becomes unstable. For the accelerated oscillator, the radiation is out of phase with the temperature in the continuous case: a small time lag is sufficient to produce a positive correlation between the radiative forcing and the temperature. In contrast, for the damped oscillator, the perturbation is in the opposite phase with the temperature in a continuous case, and the system is destabilized only for a large enough time lag, approximately half the natural period of the oscillator. This also indicates that the destabilization is not owing to the discrete aspect of the computation of the radiative heating rates. Indeed, it is well known that a linear oscillator is also destabilized by the introduction of a small time lag in the restoring force.

3. Single-column model

To explore the effects of infrequent calculation of radiation in a more realistic setting, we run a single-column model from an arbitrary initial state and follow its evolution toward radiative–convective equilibrium. The model uses the convective parameterization of Emanuel and Zivkovic-Rothman (1999) and the representation of clouds developed by Bony and Emanuel (2001). Shortwave radiative fluxes are calculated using the scheme developed by Fouquart and Bonnel (1980), while Morcrette (1991) is used for the longwave fluxes. The clouds interact fully with the radiation. The model levels are spaced at 25-hPa intervals in pressure up to 100 hPa, with nine additional levels above that. The surface is represented by a 5-m-deep slab of water whose temperature is calculated from the surface energy balance. The model is driven by annual average solar radiation at 38° latitude. For the control experiments described in this section, the radiative heating of both the surface and the atmosphere is calculated at even intervals in time, τ, and held fixed between calls to the radiation scheme. Although no internal gravity oscillations are possible in a single-column model, the convective mass flux responds to changes in environmental temperature in a manner similar to that given by (1), while the environmental temperature responds to convective mass flux as in (2). Of course, the radiation scheme is not a simple Newtonian relaxation, and the actual behavior of the convection scheme is far more complex than is represented by (1)–(3).

Figure 2 shows the behavior of the precipitation evolution for various values of τ. We regard the solution for $\tau = 1$ h as essentially the same as if radiation were called every time step; in fact, there is very little change when τ increases from 1 to 4 h. Note that the initial adjustment consists of a strongly damped oscillation with a period of around 1 day. The convective adjustment itself is strongly damped, so it is not possible to estimate a radiative relaxation rate from Fig. 2, though it is likely to be much larger than 1 day. Application of (16) would suggest that integration will be stable if $\tau < 4$–6 h.

The system has not completely reached equilibrium by the end of the integration. The small, sudden jumps in the precipitation rate evident in Fig. 2a occur when convection penetrates to a higher model level.

Comparing Figs. 2a and 2b shows a change in the character of the solution between $\tau = 4$ h and $\tau = 8$ h, and when $\tau = 12$ h, there are strong, somewhat irregular, oscillations with a period of around 3 days. In a simulation with $\tau = 24$ h (Fig. 2c), very high frequency fluctuations occur, as well as a lower-frequency modulation with a period of around 5 days.

Though nonlinearities in the model prevent instabilities from becoming catastrophic, there is clear evidence that the model is destabilized for τ greater than some critical value between 4 and 8 h. This is true even though in the single-column model there is neither wave dynamics nor advection. Thus, these simulations are likely to yield an optimistic value for the critical time interval between calls to the radiation routine.

The noisy character of the numerical simulations when τ is too large may help explain certain disparities between model simulations and measurements. For example, it is possible that the larger-than-observed variance of OLR noted by Charlock et al. (1988) may be attributable, at least in part, to the fact that radiation was calculated only every 12 h.

4. General circulation models

The interplay between large-scale flow, convection, and radiation can produce a wide variety of oscillatory behaviors that are not well captured in a single-column model. The effects of the frequency of the radiation calls are now explored in the context of an idealized general circulation model (GCM). This model uses the same physical parameterization as the single-column model discussed above, while the dynamical core is based on the Massachusetts Institute of Technology general circulation model MITgcm (Marshall et al. 1997). For simplicity, we consider only a two-dimensional (height and longitude), horizontally periodic domain in the absence of rotation. There are 40 levels, with a resolution of 25 mb, and 60 grid points in the longitudinal direction with

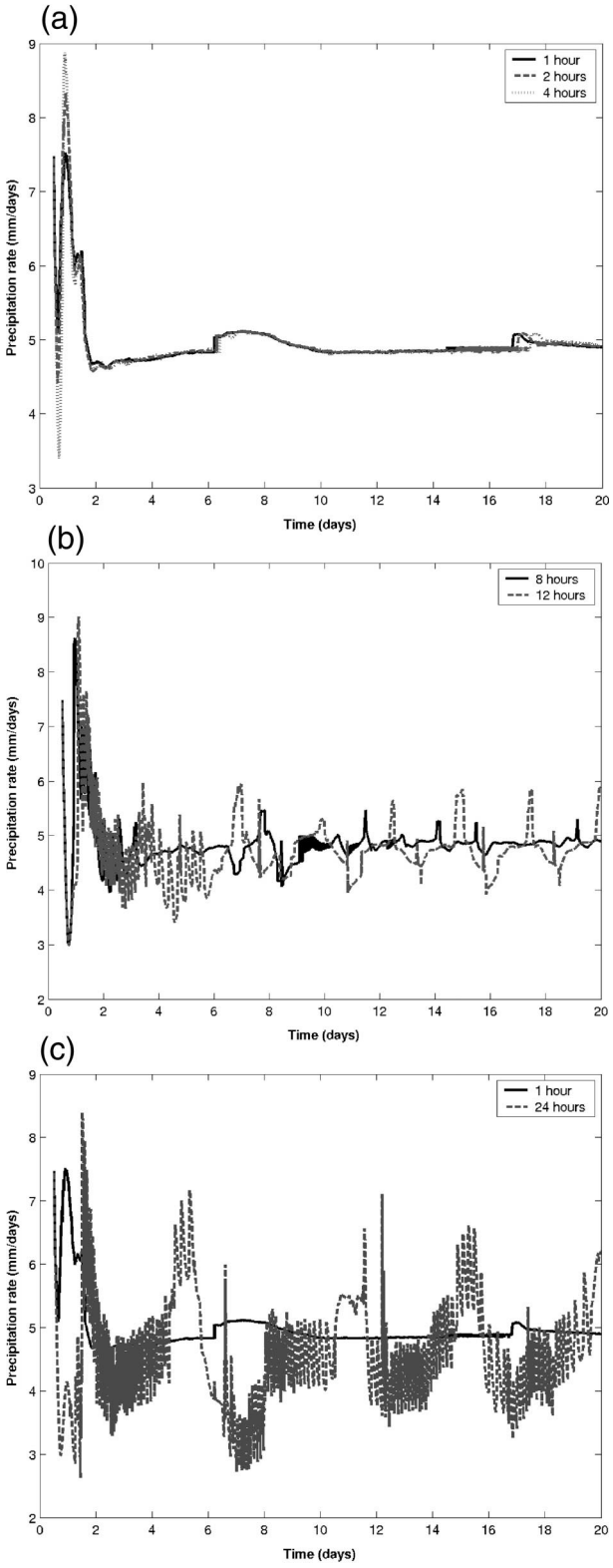

FIG. 2. Evolution with time of the precipitation rate in a single-column model, for τ = (a) 1, 2, and 4 h, (b) 8 and 12 h, and (c) 24 h. The 1-h solution is also shown in (c) for comparison.

a 1.5° resolution. The sea surface temperature is held constant at 300 K during the integrations.

a. Influence of the large-scale flow

In this model, cloud–radiative feedbacks generate localized precipitation bands that move with the mean flow, as shown in Fig. 3. These bands are present even when radiative heating rates are computed every time step. Infrequent radiation calls generate a high-frequency oscillation in the precipitation rate as shown in Fig. 4. While this behavior is similar to that of the single-column model, the oscillation is present even when the radiation field is computed every 30 min, and only disappears when the radiative heating rates are computed at every time step. For an interval of 2 h between radiation calls, the amplitude of the oscillation is about 20% of the mean precipitation, even though a 2-h interval is sufficient to ensure stability in the single-column experiment. The stability requirement for the radiation frequency depends on the large-scale circulation patterns, with regions of enhanced convection being more prone to the instability. While single-column tests can be indicative, they do not ensure the stability of a GCM.

A troubling feature of these simulations lies in that the cloud–radiative instability has a strong impact on the mean state of the atmosphere. Figure 5 shows the total outgoing longwave radiation in the equatorial band for various frequencies of radiation calls. The mean outgoing longwave radiation differs by about 15% between the run with 6-h intervals between radiation calls and the runs with more frequent updates. This decrease in OLR is due to an increase in upper-level cloudiness: the strong oscillations in the run with a 6-h interval produce thick cirrus clouds at the tropopause that greatly enhance the trapping of infrared radiation.

b. Doppler shifting and horizontal resolution

A second issue is to determine the extent to which the numerical mode can be affected by the horizontal resolution of the model, in a similar way as the dynamical time step in a GCM is usually limited by horizontal resolution and by the Courant–Friedrichs–Lewy criterion. Consider a modification to (1)–(3) that allows for horizontal advection by some constant background flow U. Then the partial time derivatives in (1) and (2) are replaced by a Lagrangian derivative:

$$\frac{\partial}{\partial t} + U\frac{\partial}{\partial x},$$

where x is a coordinate in the direction of the mean flow U. Assuming sinusoidal spatial structure with wavenumber k, it can be shown by a procedure similar to that followed in section 2 that the result is the same except replacing N by $N \pm kU$. Since the growth rate increases with the effective frequency, we will take the

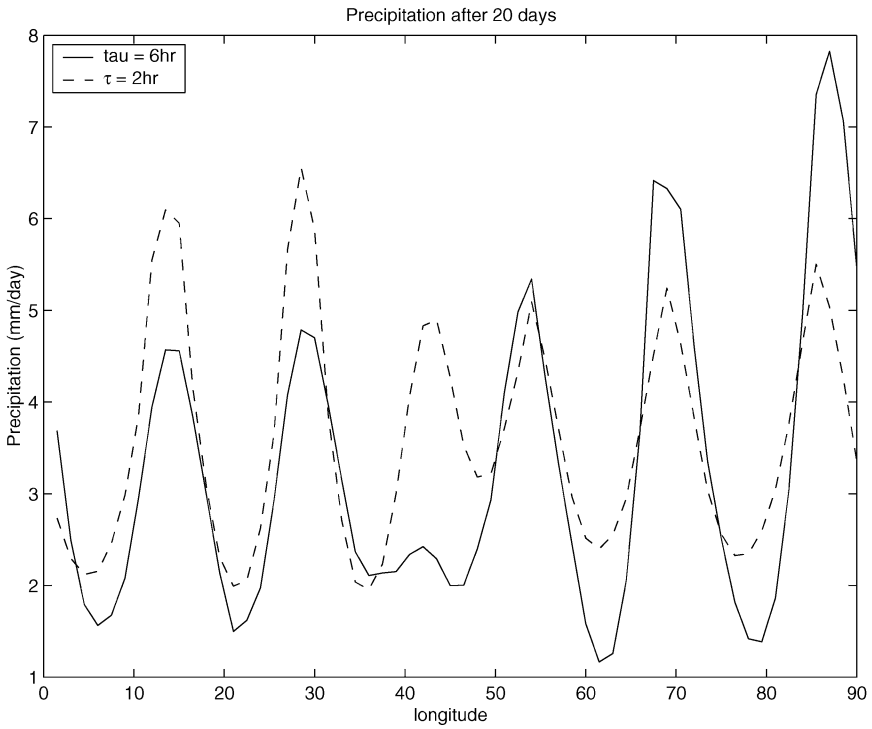

FIG. 3. Precipitation field after 20 days for a radiation frequency of 6 (solid line) and 2 h (dashed line).

greater of these two roots. Moreover, the highest wavenumber resolvable using a finite mesh is $\pi/\Delta x$, where Δx is the grid length in the x direction. Thus, using the definition

$$\Omega \equiv N + \frac{\pi U}{\Delta x}, \tag{19}$$

the discussion of section 2 applies as well, with N replaced by Ω. We note, in particular, that when $\Omega \gg \alpha$ and taking $N = 0$, we get

$$\tau < \frac{\Delta x}{U}. \tag{20}$$

This is the same criterion as that derived by Xu and Randall (1995), although the latter divided this by 2 to further enforce stability. This is a wise precaution as using a value of τ close to its critical value can distort high-frequency phenomena and introduce spurious, slowly decaying low-frequency modes. It should also be remembered that, although (27) ensures stability when the radiation acts as a damping terms on the oscillation, the undamped oscillator described in section 2a is destabilized even for the small time intervals between radiation calls.

This destabilization mechanism is tested in our numerical model by reducing the horizontal resolution to

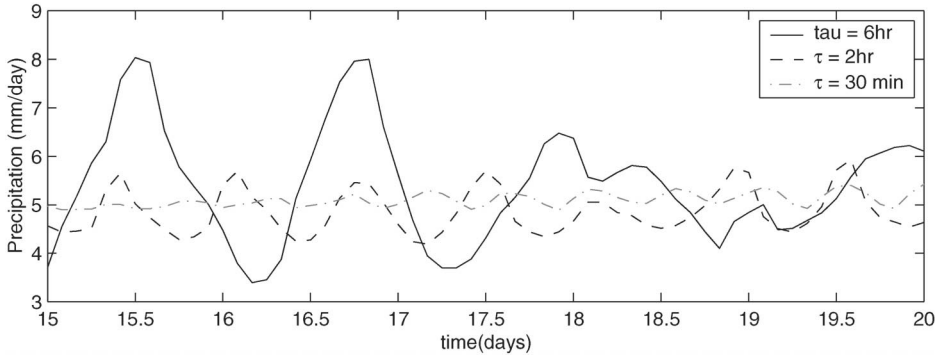

FIG. 4. Evolution of the precipitation field at one location, showing the precipitation rate for a time interval between radiation calls of 6 h (solid line), 2 h (dashed line), and 30 min (dashed–dotted line).

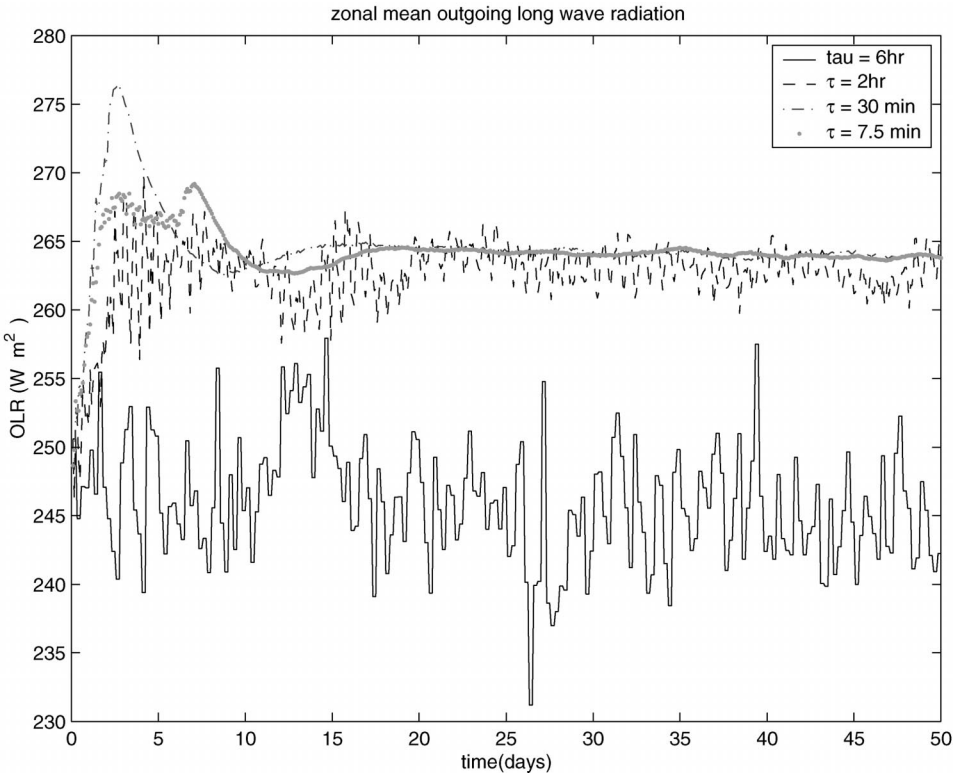

FIG. 5. Time evolution of the zonal mean OLR for time intervals between radiation calls of 6 h (solid line), 2 h (dashed line), 30 min (dashed–dotted line), and 450 s (dotted line).

0.25° and imposing a uniform zonal wind of 5 m s^{-1}. This zonal wind is kept constant in time and space. In Fig. 6, we compare the results with a time interval between radiation calls of 1 and 4 h. While the precipitation rate is uniform in the 1-h case, it exhibits high wavenumber variations in the 4-h case. In addition, in the Galilean equivalent case in which there is no zonal wind but the surface moves at 5 m s^{-1} relative to the atmosphere, the high-frequency oscillation disappears. (Note that as radiative heating rates are not advected, the Galilean invariance is lost because of the discretization of the radiation calls.)

c. *Wave propagation*

Wave propagation rather than horizontal advection is usually the limiting factor constraining the time steps in numerical models. Interactions between gravity waves and the cloud field could potentially lead to unstable oscillations as a result of infrequent radiation calls. If this is the case, the time interval between radiation calls must be shorter than the grid size divided by the propagation speed of a gravity wave c:

$$\tau < \frac{\Delta x}{c}. \tag{21}$$

As the propagation speed of the gravity waves c is usually large in comparison to the horizontal wind (at least in the tropical atmosphere), this yields a very strong constraint on the frequency of the radiation calls. However, it is possible that gravity waves might remain stable even for values of τ much larger than this critical value. This might occur, for example, because the convection scheme acts to dampen the gravity waves. Alternatively, the discussion in section 2 indicates that if the cloud–radiative feedbacks act to slow down a gravity waves, then infrequent radiation calls would not destabilize the waves.

In our idealized model, we did not find any definite evidence for the existence of an unstable ''cloud gravity'' wave. Standing oscillations similar to that discussed in section 4a are present and generate propagating gravity waves. The amplitude of the localized oscillations increases with increased resolution or with longer time between radiation calls, but we did not find any indications that the gravity waves themselves were destabilized. As this might be a fortunate coincidence resulting from the specific combination of convection and cloud schemes, one cannot rule out that for other parameterizations interactions between clouds, radiation, and gravity waves might be the lim-

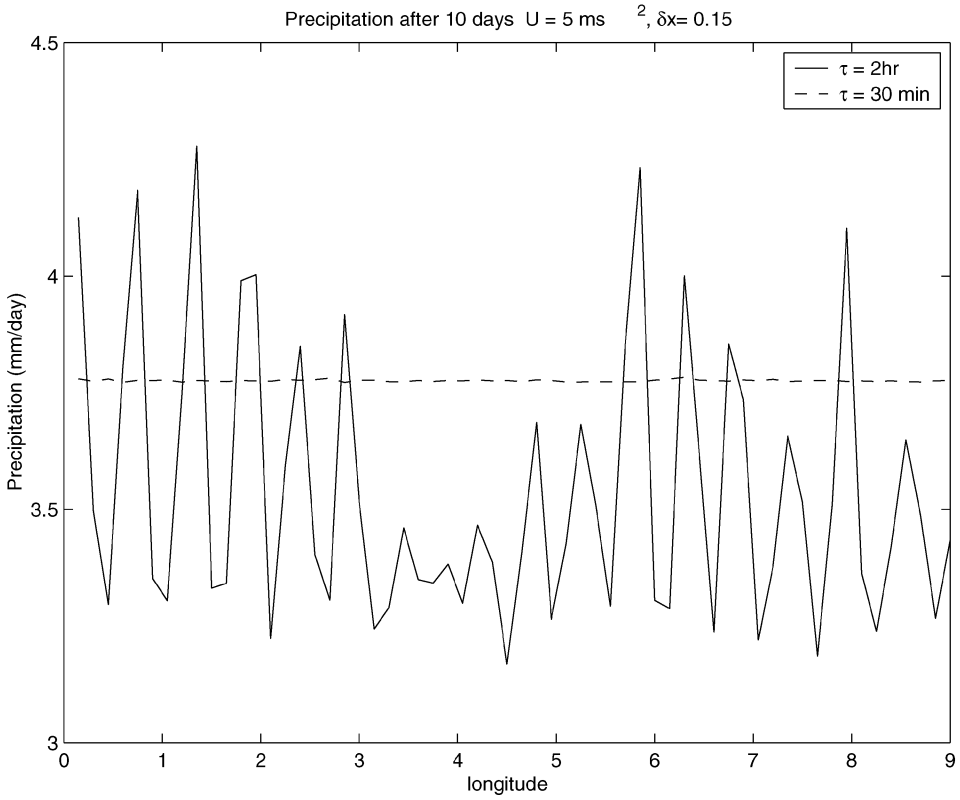

FIG. 6. Comparison between the precipitation field for a supercritical (solid line, $\tau = 2$ h) and subcritical (dashed line, $\tau = 30$ min) frequency of radiation calls, for a uniform zonal wind of -5 m s^{-1} and a grid resolution of 0.25°.

iting factor on the time interval between radiation calls.

5. Remedies

In the presence of cloud–radiative feedbacks, the radiation field cannot be treated as a slowly evolving component of the atmosphere, as infrequent calculations of the radiative heating rates can produce unstable numerical modes. It is clear from (20) that as the grid spacing of models becomes smaller and smaller, the required frequency of calls to the radiation routine becomes ever greater. In the case of cloud-resolving models, such as cumulus ensemble models, the requirement becomes very severe and is routinely violated in cumulus ensemble integrations with interactive radiation, as noted by Xu and Randall (1995), who also illustrated the types of errors that can occur in these integrations.

When it is impractical to perform full radiative transfer calculations with a frequency that satisfies (20), it would be desirable to implement some procedure that minimizes the problems that typically occur. We suggest here two alternative methods to do so.

a. Extrapolation

The numerical instability arises because the infrequent radiation calls introduce a time lag between the cloud field and its effects on radiation. One remedy to reduce the instability is to extrapolate the cloud field to half a radiation time interval later. In the linear model, this corresponds to replacing (3) by

$$R = \alpha\left(M_n + \frac{M_n - M_{n-1}}{2}\right) - \beta\left(T_n + \frac{T_n - T_{n-1}}{2}\right). \tag{22}$$

The additional terms $\frac{1}{2}(M_n - M_{n-1})$ and $\frac{1}{2}(T_n - T_{n-1})$ are the corrections resulting from a linear interpolation of the radiative forcing at time $t = (n + \frac{1}{2})\tau$. Using (22) instead of (3) reduces but does not eliminate the growth rate. More sophisticated algorithms such as a high-order Adams–Bashforth scheme (Durran 1999) can also be implemented.

We also warn the reader against using an averaging method in order to remove the instability. By averaging the radiative heating rates, one might hope to damp the high-frequency oscillations. However, in the present case, this is a very counterproductive approach that can lead to further destabilization of the lower frequencies. Indeed, replacing (3) by

$$R = \alpha\frac{M_n + M_{n-1}}{2} - \beta\frac{T_n + T_{n-1}}{2} \tag{23}$$

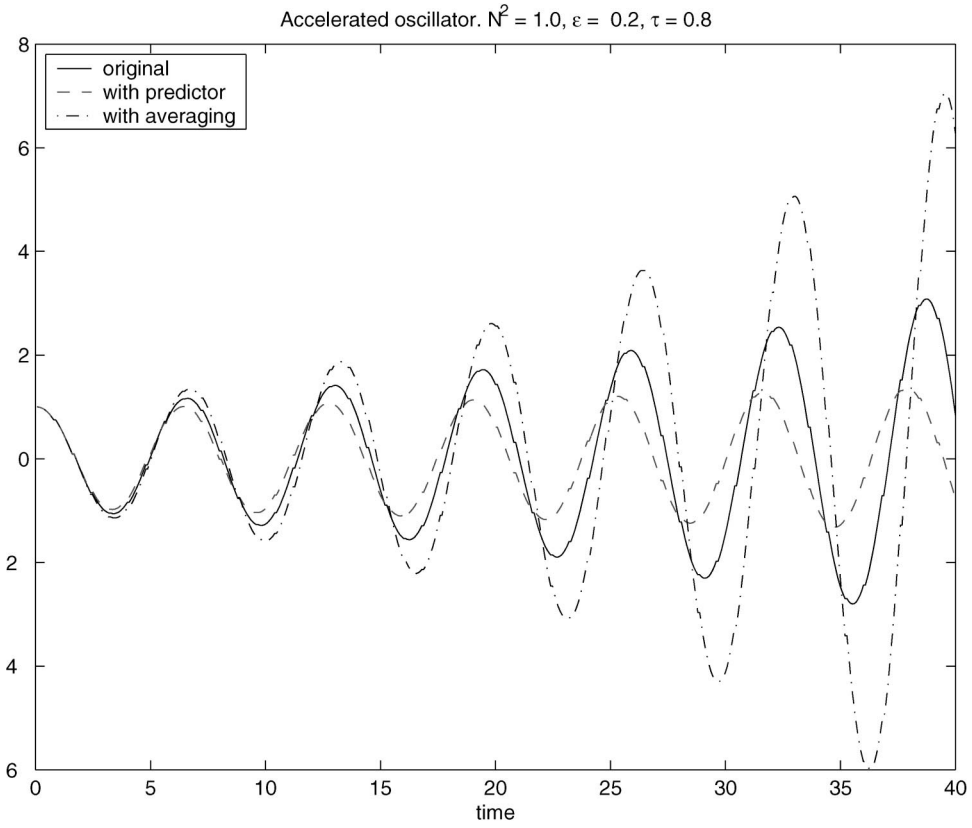

FIG. 7. Solution for the accelerated oscillator using the instantaneous value of the cloud field [Eq. (3); solid line], the predicted value of the cloud field [Eq. (22); dashed line], and the average cloud field [Eq. (23); dashed–dotted line].

is equivalent to interpolating the radiative forcing to time $t = (n - \frac{1}{2})\tau$. This increases the lag between the cloud field and radiation, and leads to a further destabilization of the oscillator.

The relative effects of extrapolation and interpolation on the linear oscillator are shown in Fig. 7. While the extrapolation method does not remove the instability, it significantly reduces the growth rate. In contrast, the averaging approach results in a more unstable system.

An important drawback of the extrapolation schemes is that they destabilize the high-frequency modes. Using (22) or one of its higher-order equivalents can only improve the simulations of oscillation with a period significantly longer that the time between two radiations calls. As the complex convective and radiative parameterizations used in the GCM can potentially generate a wide variety of oscillatory behaviors, the extrapolation method would only improve the quality of the simulations if one can be sure that all the high-frequency modes are strongly damped.

b. Reduced calculation of radiative heating

Perhaps the best way to deal with this problem is to perform some reduced calculation of the radiation at every time step, or at least frequently enough to satisfy (20). Charlock et al. (1988) suggested that a simple, linear calculation of longwave fluxes be performed in between calls to the full radiation routine. In an earlier incarnation of the ECMWF forecast model, pseudoemissivities were calculated each time the radiation scheme was called, by dividing the longwave fluxes by σT^4 in each layer; these pseudoemissivities were then multiplied by σT^4 at each subsequent time step to estimate the longwave fluxes until the next call to the full radiation scheme.

If a linear tangent of the full radiation scheme as well as its adjoint are available, one could calculate the sensitivity of radiative heating at each level within a grid column to all the relevant dependent variables at all the other model levels (and the surface) each time the radiation scheme is called. These sensitivities could then be multiplied by the departures of these dependent variables from their values at the time the radiation scheme was last called, at each subsequent time step (or every few time steps) until the full radiation is next calculated. As a crude test of such a procedure, we modify the simple linear model described in section 2 to include a simple nonlinearity. (The procedure described here would exactly reproduce the full solution of the linear

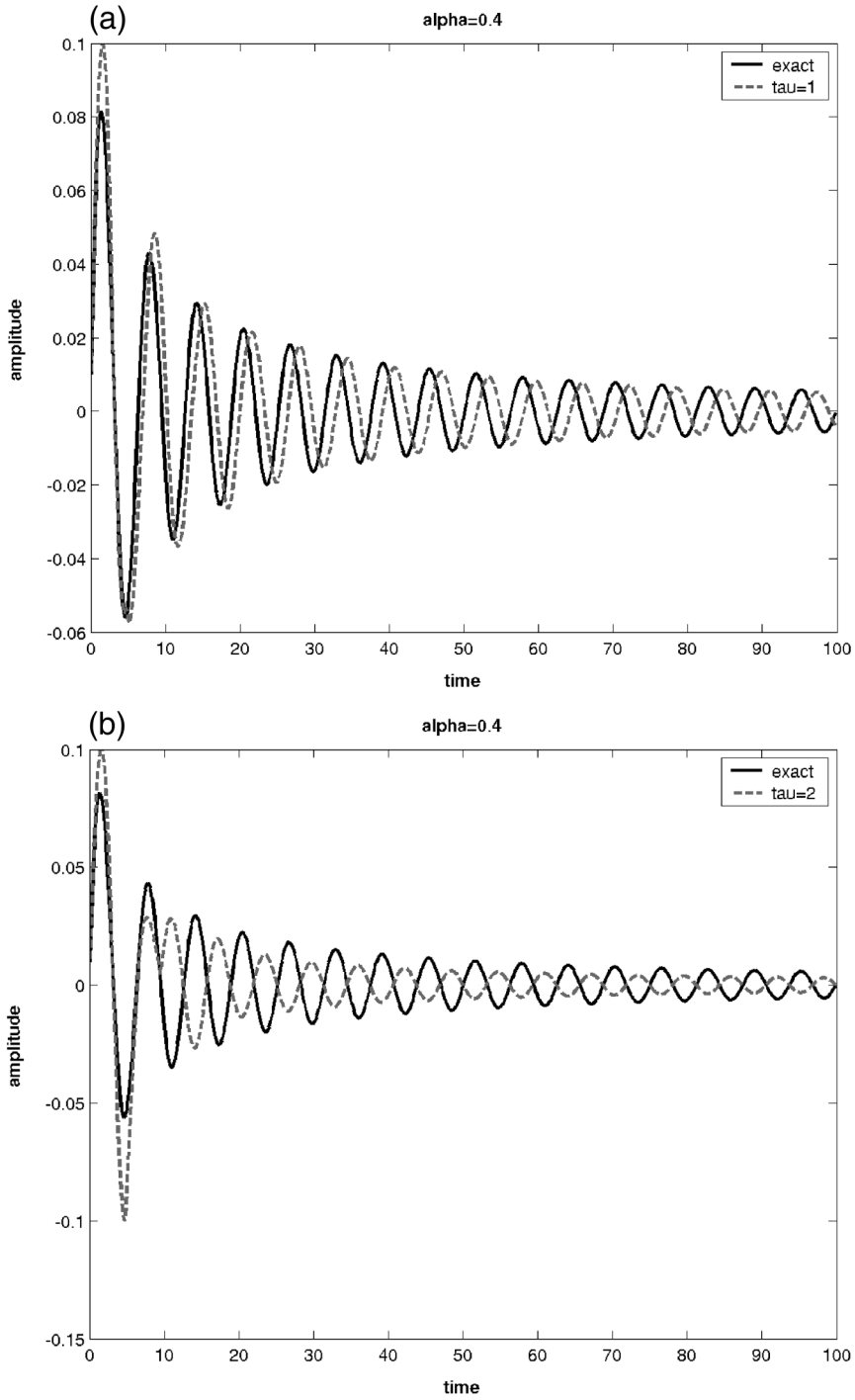

FIG. 8. Application of damping at each time step, based on linearization of the damping term at each damping interval τ, for τ approximately equal to (a) its critical value and (b) twice that value. The "exact" numerical solution is shown in both (a) and (b) for comparison.

model.) Namely, we modify (14) to include a nonlinear damping term:

$$\frac{\partial T}{\partial t} = N^2 M - \beta |T| T, \tag{24}$$

where β is a constant. Thus the damping increases with the magnitude of the perturbation. As before, we calculate the full damping term at time intervals τ, but at the same time, we calculate the linear sensitivity of the

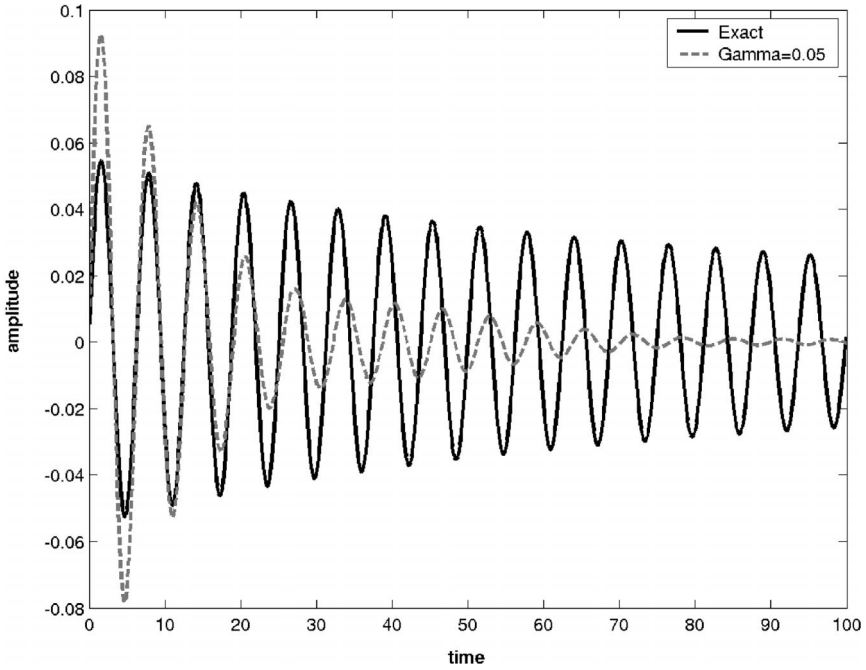

FIG. 9. Same as in Fig. 8a but for a simulation in which the calculated linear sensitivity is replaced by a constant value (0.05).

damping term to small perturbations. Denoting the damping term in (24) by D,

$$\frac{\partial D}{\partial T} = -2\beta|T|.$$

Thus, in addition to applying the constant value of the full damping term over the entire interval $n\tau \leq t < (n + 1)\tau$ as before, we also add, at each time step, the quantity

$$\frac{\partial D}{\partial T}(T - T_n), \tag{25}$$

where T_n is the value of T at the time the full damping term is calculated and $\partial D/\partial T$ is held fixed through the time interval τ.

An example of the application of this procedure is shown in Fig. 8. The ''exact'' solution of (24) (from numerical integration, applying the full damping term at every time step) is shown together with an approximate solution for two values of τ; one approximately equal to its critical value, and the second twice this value. [An exact critical value cannot be derived analytically owing to the nonlinearity of (24). For both values of τ shown, the solution is highly unstable if (25) is not applied.] Note that both the period and the amplitude of the oscillations are handled well by the procedure, though phase errors develop early in the integrations. One must expect distortions of high-frequency temperature-dependent oscillations if the radiation scheme cannot resolve them, but at least the long-term behavior is captured, and, at least in this case, no spurious low-frequency oscillations occur.

Application of this procedure to a full radiation code would result in a matrix of sensitivities in each column at each time the radiation scheme is invoked. This matrix would then be multiplied by the departures of the relevant model variables (e.g., temperature, specific humidity, and cloud variables) from their values at the time the radiation scheme was last called, at each model level. Owing to the lack of an adjoint code, we have not attempted to implement this in the single-column model discussed in section 3.

An alternative to calculating the sensitivities every time the radiation is calculated might be to use a climatological matrix of sensitivities. We test this idea first in the simple model described by (1) and (24), and then in the single-column model. For the simple model, we just replace $\partial D/\partial T$ in (25) by a constant, $-\gamma$. Otherwise, the procedure is the same as before: the full damping term is calculated every τ time units and the linear damping given by (25) is applied at each successive time step. The result, for $\gamma = 0.05$ and τ equal to its (nominal) critical value, is compared to the ''exact'' solution in Fig. 9. The oscillatory behavior is distorted compared to the case when the sensitivities are recalculated (Fig. 8a), and the decay to equilibrium is too quick, but the instability that would occur without the additional damping term is eliminated.

For the single-column model, we simply added a Newtonian damping term at each time step that relaxes the temperature and specific humidity back to their val-

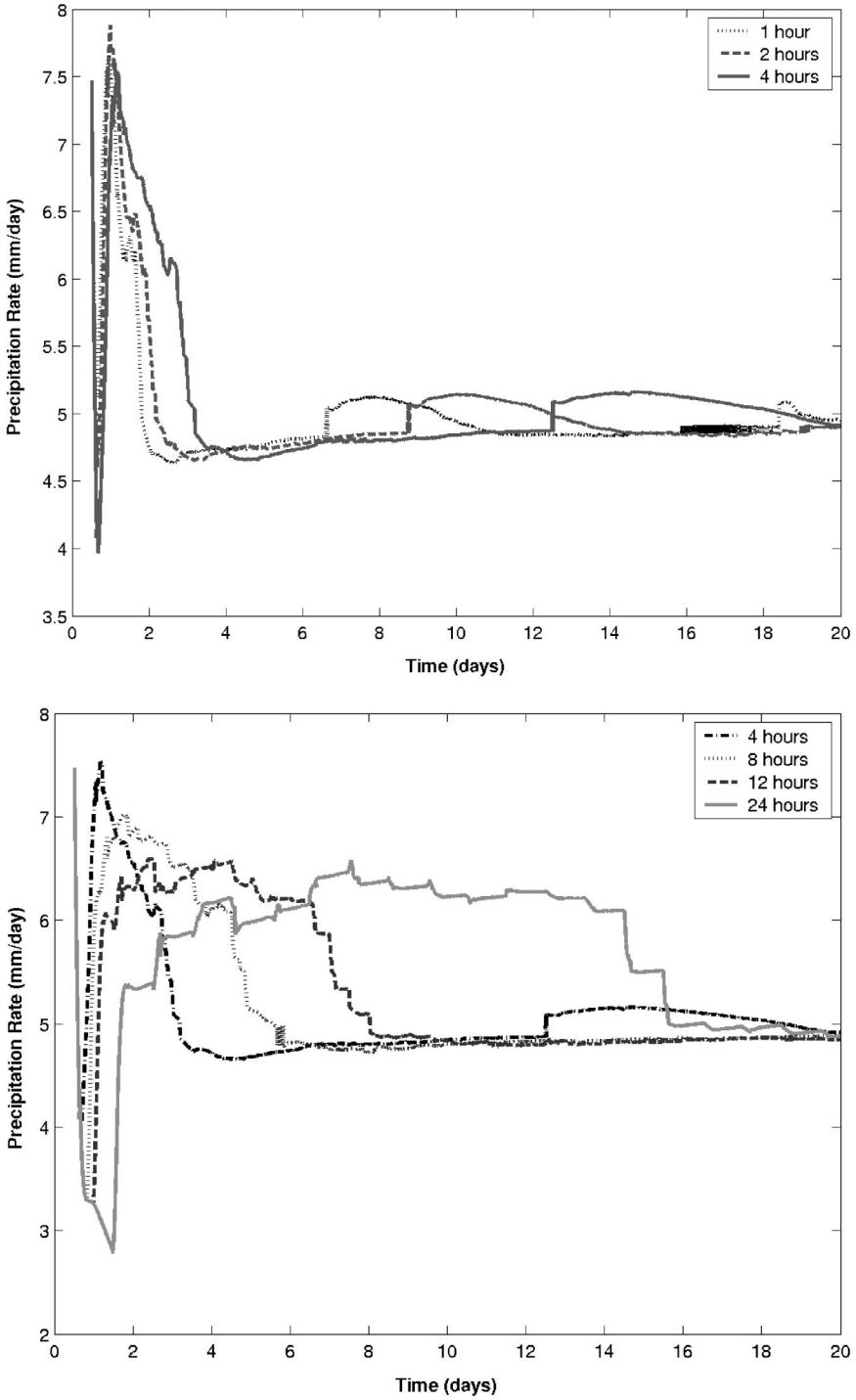

FIG. 10. Evolution with time of the precipitation rate in the single-column model, as in Fig. 2, but with linear damping applied according to (25) with a constant damping coefficient. Each curve is for a different value of τ, shown in the upper right of each panel.

ues at the last time the full radiation scheme was called, very similar to what was done in the case of the simple model just described. In the first set of experiments, this damping time scale was fixed at 1.5 h. The results are shown in Fig. 10, as a function of the time interval between calls to the radiation routine. Compared to the case where the linear damping is not applied (Fig. 2), there is little improvement and perhaps some degradation of the simulations when τ is 4 h or less. When τ is 8, 12, or 24 h, the character of the quasi-steady portion

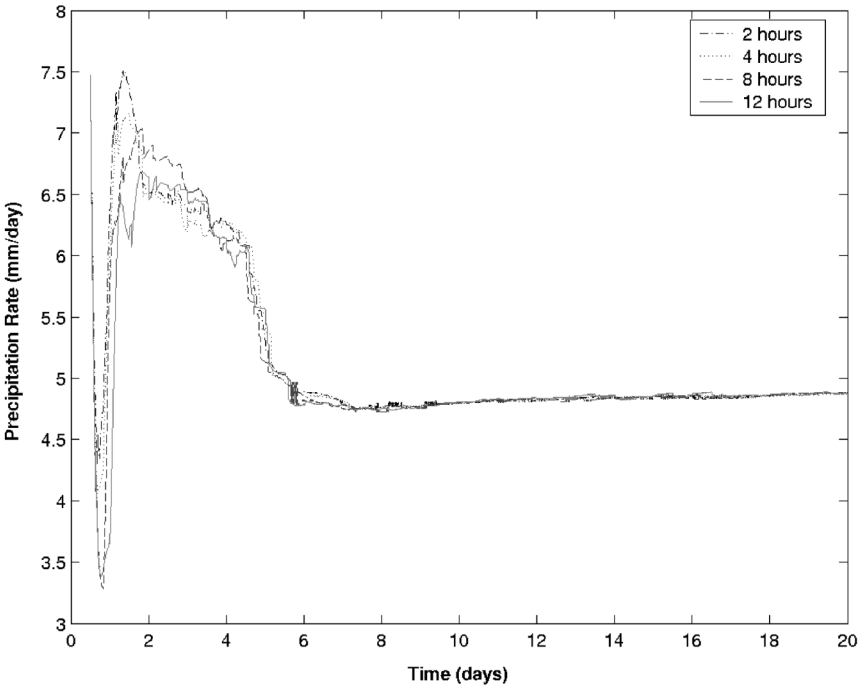

FIG. 11. As in Fig. 10 but for simulations in which the damping coefficient is inversely proportional to τ.

of the time integration is much improved, but at the expense of serious distortions of the higher-frequency variability at the beginning of the integration. In particular, the higher frequencies are damped, as one would expect, though small perturbations occur at the times the full radiation scheme is invoked.

Figure 11 shows what happens if the linear damping rate is made inversely proportional to τ (such that the damping time scale is 1.5 h when τ is 6 h). The simulations are, in this case, almost independent of the value of τ. (An experiment with $\tau = 24$ h eventually produced a steady state, but was very noisy near the beginning of the integration.) These solutions do not, however, resemble the ''exact'' solution (see Fig. 3); indeed, the limit $\tau \to 0$ is singular since the linear damping term remains finite in this limit.

Based on these limited results, it would appear that using ''climatological'' values of the sensitivity to linearly damp the model variables back to their values at the last call to the radiation scheme might buy a factor of 2 or so for the value of τ, at the expense of distorting the high-frequency response. This may be acceptable if interest is focused on the lower frequencies, or (in the case of a single-column model) if the desired result is the steady equilibrium. It would be of interest to compare these results with those obtained by calculating the matrix of sensitivities each time the radiation scheme is called.

A limitation for such a linearized approach lies in that the cloud–radiative effects are highly nonlinear, as they correspond to large variations of the emissivity at any given level associated with the appearance and disappearance of clouds. An alternative would be to compute the radiative transfer with a high-end algorithm every few hours, and then used a simpler, less accurate version to compute the evolution of the radiative heating rates on shorter time scales.

6. Summary

While it has been known for some time that numerical integrations can become distorted if the radiation is calculated too infrequently, here it is demonstrated that the time interval between the radiation calls act as a time lag that can destabilize oscillatory modes. We have shown that infrequent radiation calls produce spurious oscillations in a single-column model and in an idealized GCM. In the worst-case scenario, corresponding to the case where the cloud–radiative feedbacks act to increase the frequency of oscillations when called every time step, the artificial amplification rate is proportional to the square of the time interval between radiation calls. Experiments with various models show that high-frequency distortions and artificial, weakly damped low-frequency variability can occur for a time interval between radiation calls of a few hours, and that these oscillations can significantly alter the mean state of the atmosphere.

These distortions will usually be small under clear-sky conditions, where the variability of the radiative heating contributes little to most natural variability at these frequencies, but may be larger where radiation

interacts with clouds. In any case, to prevent artificial excitation of the high-frequency variability, some type of filtering should be applied. One possibility is to use the adjoint of the radiation code to calculate the matrix of linear sensitivities of the radiative heating to all the relevant model variables at each model level, each time the radiation scheme is called. These sensitivities can then be used to damp the model variables back toward their values at the last call to the radiation scheme. If this is not practical, the instabilities can be filtered by using climatological sensitivities in the same way.

As the destabilization mechanism is a result of the lag between the instantaneous value of the cloud field and its radiative effect, a similar instability can be produced by introducing a prognostic equation for the cloud cover. The cloud lifetime acts as a time lag between the convective activity and the radiative impact of the cloud cover. If such process plays an important role in determining the organization of convection, it is definitely preferable to have it explicitly included in the physical parameterization rather than to have it arise as a by-product of numerical discretization.

Acknowledgments. The authors thank David Randall, Jean-Jacques Morcrette, and Christian Jakob for helpful correspondence. This work was supported by NOAA Grant NA17RJ2612.

REFERENCES

Bony, S., and K. A. Emanuel, 2001: A parameterization of the cloudiness associated with cumulus convection: Evaluation using TOGA COARE data. *J. Atmos. Sci.,* **58,** 3158–3183.

Charlock, T. P., K. M. Cattany-Carnes, and F. Rose, 1988: Fluctuation statistics of outgoing longwave radiation in a general circulation model and in satellite data. *Mon. Wea. Rev.,* **116,** 1540–1554.

Durran, D. R., 1999: *Numerical Methods for Wave Equations in Geophysical Fluid Dynamcs.* Springer-Verlag, 465 pp.

Emanuel, K. A., and M. Zivkovic-Rothman, 1999: Development and evaluation of a convection scheme for use in climate models. *J. Atmos. Sci.,* **56,** 1766–1782.

Fouquart, Y., and B. Bonnel, 1980: Computation of solar heating of the earth's atmosphere: A new parameterization. *Beitr. Phys. Atmos.,* **53,** 35–62.

Marshall, J., A. Adcroft, C. Hill, L. Perelman, and C. Heisey, 1997: A finite-volume incompressible Navier–Stokes model for studies of the ocean on parallel computers. *J. Geophys. Res.,* **102,** 5753–5766.

Morcrette, J.-J., 1991: Radiation and cloud radiative properties in the European Centre for Medium-Range Weather Forecasts forecasting system. *J. Geophys. Res.,* **96,** 9121–9132.

——, 2000: On the effects of the temporal and spatial sampling of radiation fields on the ECMWF forecasts and analyses. *Mon. Wea. Rev.,* **128,** 876–887.

Xu, K.-M., and D. A. Randall, 1995: Impact of interactive radiative transfer on the macroscopic behavior of cumulus ensembles. Part I: Radiation parameterization and sensitivity tests. *J. Atmos. Sci.,* **52,** 785–799.